Determination of Landau free-energy parameters by dielectric measurements in the ferroelectric TSCC

Authors: J. Bornarel & V. Hugo Schmidt

Determination of Landau free-energy parameters by dielectric measurements in the ferroelectric TSCC

J Bornarel and V H Schmidt†

Université Scientifique et Médicale de Grenoble, Laboratoire de Spectrométrie Physique (associé au CNRS), Boîte Postale no 53X 38041 Grenoble Cedex, France

Abstract. We measured the adiabatic dielectric permittivity ε_b of tris-sarcosine calcium chloride (TSCC) at 400 Hz near the ferroelectric transition for DC bias fields up to 5000 V cm^{-1}. We found $\varepsilon_\infty = 4.2 \pm 0.2$, Curie–Weiss constant $C^+ = 38.3 \pm 0.3$ K, $T_0 = 129.4 \pm 0.1$ K, and Landau coefficients $A = (2.95 \pm 0.2) \times 10^9$ V m A^{-1} s^{-1} K^{-1} and $B = (3.5 \pm 0.1) \times 10^{15}$ V m^5 A^{-3} s^{-3}. We observed evidence of an internal bias field as reported previously by others.

1. Introduction

Tris-sarcosine calcium chloride (TSCC) has a paraelectric (PE) to ferroelectric (FE) transition near 130 K. Its structure was found (Ashida *et al* 1972) to be orthorhombic Pnma in the PE phase, with $Z = 4$ formula units of $(CH_3NHCH_2COOH)_3CaCl_2$ per unit cell. The FE phase is presumed (Makita 1965) to remain orthorhombic, with space group Pn2$_1$a and $Z = 4$. Dielectric investigations of TSCC have already been made by several groups. Such studies at high pressure have partly elucidated the phase diagram. The PE–FE transition temperature T_c increases rapidly with pressure (Windsch and Schmidt 1979, 1980). At higher pressure a disappearance (Hegenbarth and Schmidt 1980, Fujimoto *et al* 1980) of the dielectric anomaly was noted. This disappearance was found (Schmidt 1980) to coincide with a transition to a third, probably antiferroelectric (AFE), phase which exists only at high pressure, the common point for the three phases being at 5.03 kbar and 176.8 K. The most extensive dielectric measurements have been made at ambient pressure. The effects of temperature and DC electric field were studied (Makita 1965, Levstik *et al* 1975, Sorge and Straube 1979). The latter authors investigated also the effect of the amplitude and frequency of the measuring field and reported unusual results for the effect of a DC field E on the dielectric permittivity ε_b: 'For E smaller than 0.5 kV cm^{-1} the maximum of ε_b is shifted to lower temperatures, whereas for E greater than 0.5 kV cm^{-1} it is shifted to higher temperatures with $dT_c/dE = 0.18 \pm 0.02$ K cm kV^{-1}. The shift at low field also depends on the sign of E'.

The purpose of the present work was:

(i) to clarify if possible this behaviour of $\varepsilon_b(E, T)$;

† Permanent address: Department of Physics, Montana State University, Bozeman, Montana 59717, USA.

(ii) to determine precisely the coefficients of the Landau free-energy expansion from dielectric measurements.

2. Experimental

The first sample was taken from a crystal grown by us by the evaporation method from aqueous solution of 98% pure sarcosine and calcium chloride. The second and third samples were from recrystallised TSCC crystals and presumably have higher purity. TSCC crystals generally grow with ferroelastic twins (domains) (Sawada *et al* 1977) which are observable under a polarising microscope for light propagating along the *a* axis. Mono-domain portions were cleaved from these crystals and replaced in solution, after which they generally remained monodomain during further growth. Our samples were made from such ferroelastically monodomain crystals by polishing them with wet filter paper to parallelepiped shape with faces perpendicular to crystallographic axes. Dimensions were $a = 3.25$ mm, $b = 2.15$ mm, $c = 5.95$ mm for the third sample, for which the quantitative results reported herein were measured. Gold electrodes were deposited by evaporation on the faces perpendicular to the FE *b* axis. Electrical contacts to the samples were made by two methods.
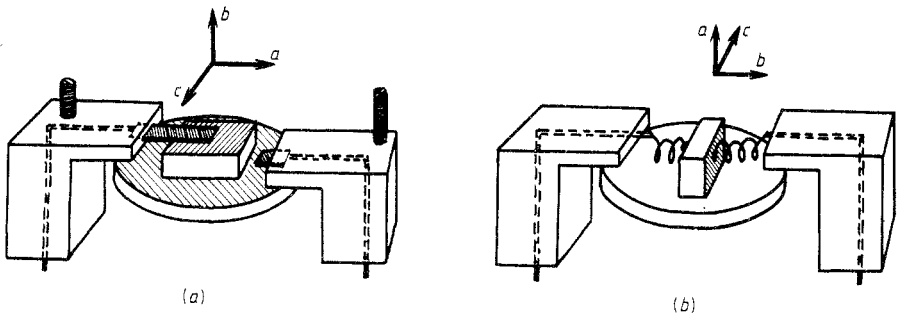

Figure 1. (*a*) First method for providing electrical contacts to crystal. (*b*) Second method for providing electrical contacts to crystal.

In the first method, used with the first two samples and shown in figure 1(*a*), the sample was placed on a metallised support. Its upper face was contacted by a copper foil attached to a Teflon block whose position was adjustable to give the desired contact pressure. Spots of silver paste assured good contact of the crystal electrodes to the support plate and the copper foil. A disadvantage of this method is that differential thermal expansion may cause excessive compression along *b* at low temperature.

In the second method, illustrated in figure 1(*b*) and employed for the third sample, a face perpendicular to *a* rested on an insulating block. Contacts were made by very weak beryllium–copper coil springs attached to the *b* faces by drops of silver paint, thus achieving a very weak and nearly temperature-independent compressive force along *b*.

The samples were placed in a cell designed for electrical measurements and optical viewing. Temperature was regulated by a heater located on the thermal path between the crystal and a liquid nitrogen reservoir. Helium at low pressure acted as an exchange gas to maintain essentially uniform sample temperature despite radiation losses through

the viewing window. A Eurotherm type 040 temperature regulator provided stability of 10^{-2} K or better, as measured with a Rosemount platinum resistor and a Dana 5000 digital multimeter readout. The relative precision of two measurements near T_c was of order 0.01 K, but the absolute accuracy was only several tenths of a degree.

The dielectric measurements were performed at 400 Hz and 1 V RMS with a General Radio type 1673 automatic capacitance bridge. The precision for C was 0.05 pF, and for tan δ varied from 0.05 for low values of C near room temperature to 0.001 near the transition. An appropriate circuit permitted application of DC voltages up to ± 1000 V to the crystal while isolating the measuring bridge from this DC voltage.

The experimental procedure consisted in measuring the dielectric permittivity $\varepsilon_b(E, T)$ at a fixed temperature T for all of the desired bias-field values E, then repeating the process at other temperatures near T_c. The temperature was regulated for several hours at each new value before beginning dielectric measurements, to ensure thermal homogeneity of the sample. Then ε_b (at 400 Hz and 1 V RMS) was monitored after each stepwise change in E until it had remained constant for several minutes, at which time its value was recorded. This procedure eliminated possible errors resulting from transient adiabatic temperature changes of the sample caused by changes in E, changes which would not be noted by the resistance thermometer which was nearby but did not touch the sample. In fact, however, the new values of C and tan δ generally stabilised within a few seconds after the step change in E.

3. Results

The most readily apparent result is the asymmetry relative to applied field of the real part $\varepsilon_b'(E)$, of the permittivity. All three samples exhibited at fixed $T \simeq T_c$ a sharp peak of $\varepsilon_b'(E)$ displaced from $E = 0$. In addition, the first two samples exhibited a rounded side peak of $\varepsilon_b'(E)$ for one polarity only of E. Both of these samples were mounted as shown in figure 1(a); one was from a crystal grown from the original solution while the other was from a recrystallised crystal. Accordingly, non-uniform compressive stress rather than crystal perfection seems to govern this asymmetric behaviour.

The third sample whose mounting system shown in figure 1(b) caused weaker forces, exhibited no side peak; its $\varepsilon_b'(E)$ form was symmetric with respect to a positive field value which gave maximum ε_b'. Such curves for five temperatures near T_c are shown in figure 2; the highest value of ε_b' (more than 1700) is obtained for a temperature of 130.54 K and a field E_m of 45 ± 5 V cm^{-1}, no effect of T on the field E_m giving maximum ε_b' is really noticeable.

The results can also be plotted in the form $\varepsilon_b'(T)$ for various bias fields as shown in figure 3. First we note that the temperature $T_m(E)$ giving maximum ε_m' decreases up to $E \simeq E_{bias} = 45 \pm 5$ V cm^{-1} and then increases monotonically for larger E. A similar effect was observed previously (Sorge and Straube 1979) as noted in the Introduction, except that the internal bias field apparently was about 11 times larger than ours. Although $T_m(E)$ is expected to be a non-linear function of E as explained in the Appendix, we can note that T_m increases by 0.61 ± 0.06 K as E increases from 0.14 to 4.65 kV cm^{-1}, which is comparable with the result $dT_m/dE = 0.18 \pm 0.02$ K cm kV^{-1} quoted previously (Sorge and Straube 1979).

Finally we note that the peak value of ε_b' first increases with E and is largest for the 46.5 V cm^{-1} curve, after which it decreases monotonically with increasing E. The peak becomes broad and ill-defined at the highest fields used.
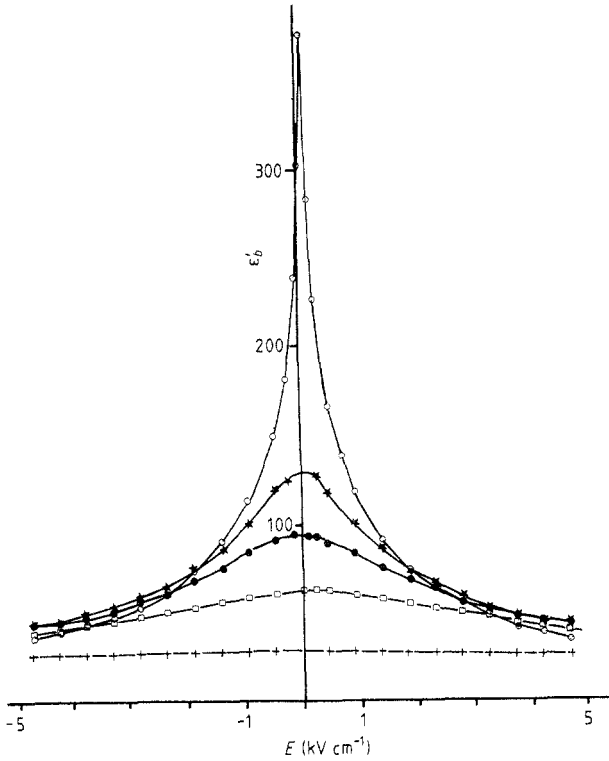
Figure 2. AC (adiabatic) permittivity ε_b' versus applied DC field E at five temperatures ; ($\bigcirc$) = 130.764 ± 0.005 K, ($\bullet$) = 130.94 ± 0.01 K, ($\bullet$) = 131.07 ± 0.01 K, ($\square$) = 131.33 ± 0.01 K, (+) = 132.055 ± 0.002 K. Note displacement caused by effective internal bias field of −45 ± 5 V cm^{-1}.

4. Discussion

We analyse our results in terms of the Landau–Devonshire free energy

$$F = \tfrac{1}{2}A_0tP^2 + \frac{1}{2n}B_{2n}P^{2n} - EP \tag{1}$$

in which P is the polarisation, $t = T - T_0$ with T_0 being the Curie–Weiss temperature which is also T_c for non-first-order transitions as studied here, and A_0 and B_{2n} are positive constants. If $n = 2$ we have a second-order transition while if $n = 3$ the transition is at a tricritical point.

From the development based on equation (1) given in the Appendix it is easy to see that the variations of $1/\varepsilon_m'$ and t_m with field E allow determination of n and B_{2n} if only one P^{2n} term plays a preponderant role as assumed in equation (1).

We accordingly made the logarithmic plot of $1/\varepsilon_m'$ versus E shown in figure 4. Between 1 and 5 kV cm^{-1} the slope is 2/3 as predicted for $n = 2$, so that no terms of order higher than P^4 in the free energy are necessary in the range of E and T covered in this experiment.
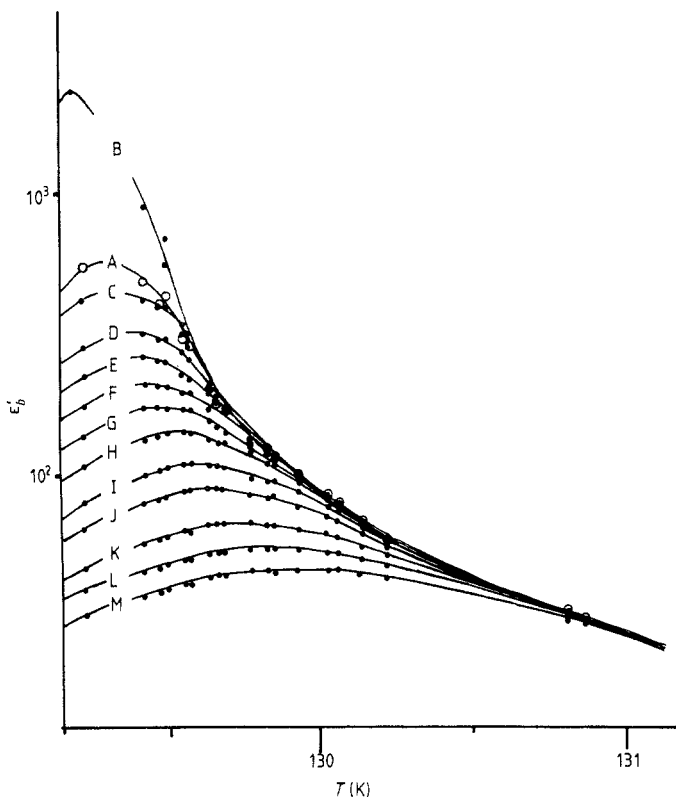
Figure 3. AC (adiabatic) permittivity ε_b' versus temperature T for thirteen applied DC fields having magnitudes in V cm^{-1} of 0 (A), 46.5 (B), 139.5 (C), 232.6 (D), 325.6 (E), 465 (F), 651.2 (G), 930.2 (H), 1395 (I), 1860 (J), 2791 (K), 3721 (L), 4651 (M). Note that highest peak occurs for curve B for which the applied field apparently cancels the internal bias field.
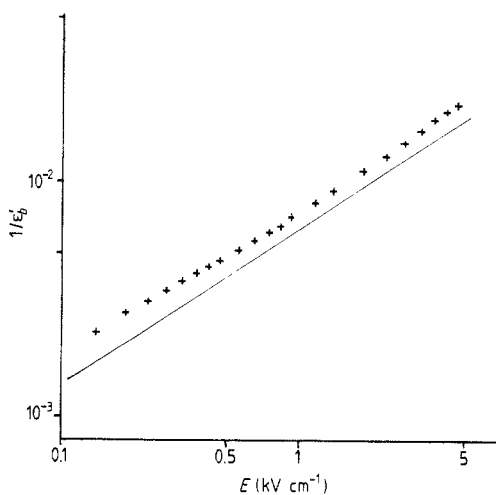

Figure 4. Logarithmic plot of inverse of peak adiabatic permittivity $(\varepsilon_m')^{-1}$ versus applied field E, with line of slope 2/3 for comparison.

It remains to determine $A_0 T_0$, and B_4 (henceforth called B) in equation (1). To find A_0 and T_0 we use the law

$$\varepsilon_b' = \varepsilon_\infty' + C^+/(T - T_0)$$

in the form $A_0(T - T_0) = (\varepsilon_b' - \varepsilon_\infty')^{-1}$ where $C^+ = (A_0 \varepsilon_0)^{-1}$. Then a plot of $(\varepsilon_b' - \varepsilon_\infty')^{-1}$ versus T yields A_0 as the slope and T_0 as the intercept. We find $\varepsilon_\infty' = 4.2 \pm 0.2$, $C^+ = 38.3$ K, $A_0 = (2.95 \pm 0.2) \times 10^9$ V m A^{-1} s^{-1} K^{-1} and $T_0 = 129.4 \pm 0.1$ K. To find B we plotted $(1/\varepsilon_m')^{3/2}$ as a function of E in figure 5, for which the slope is proportional to $B'^{1/2}$ as shown in the Appendix. After subtracting the adiabatic correction $B' - B$, we found $B = (3.5 \pm 0.1) \times 10^{15}$ V m^5 A^{-3} s^{-3}.
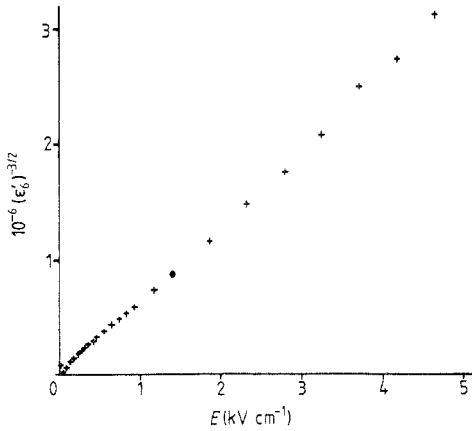

Figure 5. Plot of $-3/2$ power of peak adiabatic permittivity, $(\varepsilon_m')^{-3/2}$, versus applied field E, having slope proportional to Landau coefficient B plus an adiabatic correction term ($B' - B$).

The other law developed in the Appendix, giving $t_m = T_m - T_0$ as a function of E, is much less precise experimentally for two reasons. First, T_0 is not known precisely enough, and second, t_m is difficult to establish exactly from figure 3. By way of contrast, T_0 does not appear in the $\varepsilon_m'(E)$ law and ε_m' can be measured much more precisely than t_m. Nevertheless, the law $t_m = 3B'^{1/3} 4^{-2/3} A_0^{-1} E^{2/3}$ using the values of A_0 and B' found above is in approximate agreement with experiment.

The above method is equally useful for calculating the coefficient C (or B_6 here) of the P^6 term in the free energy if that term becomes predominant over the P^4 term. The slope in figure 4 then becomes 4/5 instead of 2/3, as was found experimentally (Bornarel and Troussaut) for KH$_2$PO$_4$ for applied fields above 4 kV cm^{-1}. For TSCC the $\frac{1}{6}CP^6$ term with the value of C found previously (Sorge and Straube 1979) contributes only a few per cent at the right side of figures 4 and 5, and fields above 80 kV cm^{-1} would be necessary to make this term predominate!

Values found by various workers for A_0, B and C are shown in table 1. There is a large variation in values of A_0 whose origin is not clear. The value of B differs from those found by others (Makita 1965, Sorge and Straube 1979), but their values were found from the spontaneous polarisation curve values assuming that B is independent of temperature over a wide temperature range, while our B is determined from measurements near T_c. Our method not only has this advantage of determining B (or C) over a

narrow temperature range; it also does not require previous or simultaneous determination of A_0 and T, except in determining the adiabatic correction. The fractional adiabatic correction $(B' - B)/B$ is rather small (0.173) for TSCC; for crystals like KH_2PO_4 in which it is about 50 times larger (Western and Schmidt 1976), isothermal susceptibility values would be necessary for accurate determinations of B by the method presented in the Appendix.

Table 1. Free-energy parameters A_0, B and C for TSCC.

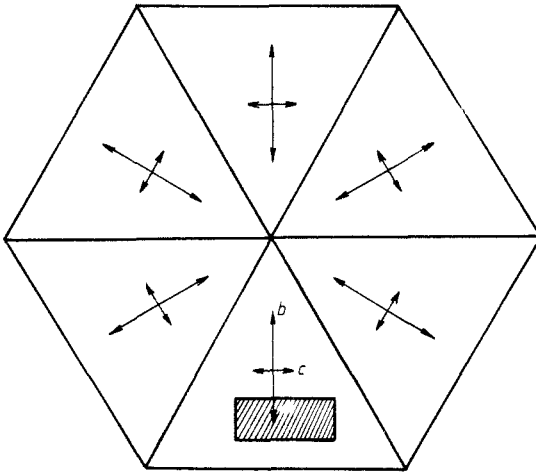| Reference	A_0 $(10^9 \text{ V m A}^{-1}\text{s}^{-1}\text{K}^{-1})$	B $(10^{15} \text{ V m}^5 \text{ A}^{-3}\text{s}^{-3})$	C $(10^{21} \text{ V m}^9 \text{ A}^{-5}\text{s}^{-5})$
Makita (1965)	1.9 ± 0.1	4.6 ± 0.4	
Levstik *et al* (1975)	6.61		
Sorge and Straube (1979)	1.94 ± 0.04	4.4 ± 0.1	1.4 ± 0.2
Fujimoto *et al* (1980)	2.98		
Schmidt (1980)	3.65 ± 0.2		
This work	2.95 ± 0.1	3.5 ± 0.1	

Figure 6. Sketch of projection along *a* axis of typical ferroelastically polydomain TSCC crystal, showing *b* axis direction for monodomain portion cleaved from this polycrystal. The asymmetry along *b* could give rise to defect or impurity gradients which could cause the observed effective internal bias fields.

Several questions remain open after these measurements. First, what is the origin of the internal bias field observed by us and others (Sorge and Straube 1979)? Further studies are desirable with crystals having various concentrations of impurities, taking into account also the relation between the sign of the bias field and the direction of the surface perpendicular to *b* of the ferroelastic monodomain cleaved from the parent polydomain crystal, as shown in figure 6. In this connection, optical viewing along the

a axis during application of DC fields is desirable to ensure that the fields do not create new ferroelastic domains in the originally monodomain samples.

A second question is the origin of the downturn of the $(1/\varepsilon'_m)^{3/2}$ versus E curve in figure 4 at small $1/\varepsilon'_m$. One would expect a rounded minimum resulting from a defect-induced distribution of T_c's rather than the observed pointed minimum.

Finally, what is the effect of pressure on B? Does it remain positive up to the three-phase common point at 5.03 kbar (Schmidt 1980), corresponding to the PE–FE transition remaining of second order? Similar measurements under hydrostatic pressure are desirable to answer this question.

Acknowledgments

Appendix

We present here a calculation of ε'_m and t_m as functions of E, for a Landau free energy of the form

$$F = \tfrac{1}{2}A_0 t P^2 + \frac{1}{2n} B_{2n} P^{2n} - EP, \tag{A1}$$

where $t = T - T_0$, and ε'_m and t_m are for a given field E the maximum real dielectric permittivity and the temperature (less T_0) at which this maximum occurs. By differentiation one obtains the equation of state

$$E = A_0 t P + B_{2n} P^{2n-1}, \tag{A2}$$

which after a second differentiation yields the inverse isothermal susceptibility

$$\chi_T^{-1} = A_0 t + (2n - 1) B_{2n} P^{2n-2}. \tag{A3}$$

Since we are looking for ε'_m and t_m for curves of fixed DC field E, the total derivative of equation (A2) yields

$$dP/dt = -A_0 P/[A_0 t + (2n - 1) B_{2n} P^{2n-2}]. \tag{A4}$$

The maximum χ_T occurs where

$$d\chi_T^{-1}/dt = A_0 + (2n - 1)(2n - 2) B_{2n} P^{2n-3} dP/dt = 0. \tag{A5}$$

Substitution of equation (A4) into equation (A5) yields

$$A_0 t_{mT} = (2n - 1)(2n - 3) B_{2n} P_m^{2n-2}, \tag{A6}$$

which together with equations (A2) and (A3) yields

$$t_{mT} = 3B^{1/3} E^{2/3}/2^{4/3} A_0, \tag{A7}$$

$$\chi_{mT}^{-1} = 3B^{1/3} E^{2/3}/2^{1/3}, \tag{A8}$$

for $n = 2$ and $B_{2n} = B$ as required for our analysis. The approximation $= 1 + \chi/\varepsilon_0 \simeq \chi/\varepsilon_0$ is sufficiently accurate for this study. Because our measurements were

made at 400 Hz, we determined the adiabatic susceptibility χ_S, which is related to χ_T by

$$\chi_S^{-1} = \chi_T^{-1} + TC_P^{-1}[(\delta E/\delta T)_P]^2, \tag{A9}$$

(Jona and Shirane 1962), where C_P is specific heat per unit volume at fixed P. Using equations (A2) and (A3) we obtain

$$\chi_S^{-1} = A_0 t + (3B + TA_0^2/C_P) P^2 \tag{A10}$$

for the $n = 2$ case. From here on we will suppress the subscript S. With χ_T^{-1} replaced by this χ_S^{-1} in the foregoing analysis, equation (A6) becomes

$$A_0 t_{\rm m} = 3BP_{\rm m}^2 + 2A_0 T_0 P_{\rm m}^2/(C_P - A_0 P_{\rm m}^2), \tag{A11}$$

but the $AP_{\rm m}^2$ term in the denominator can be neglected because $A_0 P_{\rm m}^2/C_P = 0.0003$ for the largest field used in this study. Then the analysis proceeds as before, giving

$$E = 4B(1 + T_0 A_0^2/2C_P B) P_{\rm m}^3 = 4B' P_{\rm m}^3. \tag{A12}$$

Using the fact that for TSCC a binomial expansion of the factor in parentheses is justified, we find that the equivalents of equations (A7) and (A8) for adiabatic $t_{\rm m}$ and $\chi_{\rm m}^{-1}$ have the same form but with B replaced by B'. The value of $B' - B$ is 0.606×10^{15} V m^5 A^{-3} s^{-3}, where C_P is calculated using the heat capacity per unit volume of 55 cal mol^{-1} K^{-1} just above T_c (Makita 1965) and the density of 1.53 g cm^{-3} quoted (Ashida et al 1972) for TSCC.

References

Ashida T, Bando S and Kakudo M 1972 *Acta Crystallogr.* B28 1560
Fujimoto S, Yasuda N, Takagi K, Narayanan P S and Bhat H L 1980 *J. Phys. D: Appl. Phys.* 13 L107
Hegenbarth E and Schmidt B 1980 *Ferroelectrics* 25 359
Jona F and Shirane G 1962 *Ferroelectric crystals* (New York: Pergamon) p 39
Levstik A, Filipič C and Blinc R 1975 *Solid State Commun.* 18 1231
Makita Y 1965 *J. Phys. Soc. Japan* 20 2073
Sawada A, Makita Y and Takagi Y 1977 *J. Phys. Soc. Japan* 42 1918
Schmidt V H 1980 *Solid State Commun.* 35 649
Sorge G and Straube U 1979 *Phys. Stat. Solidi* (a) 51 117
Western A B and Schmidt V H 1976 *Solid State Commun.* 19 885
Windsch W and Schmidt V H 1979 *Bull. Am. Phys. Soc.* 24 507
——1980 *Ferroelectrics* 30 to appear